NASA Contractor Report NASA/CR-2003-211192

MiniSODAR™ Evaluation

Prepared by:
The Applied Meteorology Unit

Prepared for:
Kennedy Space Center
Under Contract NAS10-01052

NASA
National Aeronautics and
Space Administration

Office of Management

Scientific and Technical
Information Program

2003

Attributes and Acknowledgements

NASA/KSC POC:
Dr. Francis J. Merceret
YA-D

Applied Meteorology Unit (AMU) / ENSCO Inc.
David A. Short
Mark M. Wheeler

Executive Summary

The goal of this study was to determine the quality of wind speed and direction data from the Doppler MiniSODAR™ System (DmSS, from AeroVironment, Inc.) near Space Launch Complex 37 (SLC-37). The DmSS is an acoustic wind profiler that uses Doppler, SODAR (SOund Detection And Ranging) and phased-array technologies to determine wind speed and direction over the height interval from ~50 to ~410 ft. The Boeing Company installed a DmSS near SLC-37 in mid-2002 as a substitute for a tall wind tower and plans to use the DmSS data for the analysis and forecasting of winds for the new Evolved Expendable Launch Vehicle during ground and launch operations. Peak wind speed data are of particular importance for evaluating Launch Commit Criteria (LCC). In order to make critical GO/NO GO launch decisions, Launch Weather Officers (LWOs) and forecasters from the 45th Weather Squadron (45 WS) need to know the quality and reliability of DmSS data, especially as it applies to peak wind speeds.

The Applied Meteorology Unit obtained data from the SLC-37 DmSS and nearby wind towers on a monthly basis from August 2002 to July 2003 and performed a comparative analysis of data availability, average wind speed and direction, and peak wind speed between the towers and the DmSS.

The results from this study are summarized as follows:

- The overall DmSS data availability at the 98 ft level, the level to be monitored by the Launch Weather Officer during operations, averaged 90% or better. There was a decrease in data availability with height, falling to 85% or less at 300 ft, consistent with previous DmSS studies. There was a distinct diurnal cycle in DmSS data availability with a ~15% reduction for several hours around sunrise and sunset. Precipitation also resulted in missing data from the DmSS.

- The DmSS vertical profile and diurnal cycle of average wind speed showed good agreement with the wind towers. The performance of the DmSS in measuring the average wind speed and direction was consistent with previous studies of Doppler/SODAR instruments. Variations in wind speed and direction associated with weather phenomena such as sea breezes were detected well by the DmSS and the towers. Comparisons of 5-minute wind speeds between the DmSS and wind towers showed some differences, but the differences were not greater than what could be attributed to turbulent variations in the wind field.

- The DmSS peak wind speeds were higher, on average, than the wind tower peak wind speeds by about 25%. The vertical profile of DmSS peak wind speeds showed a consistent over-estimate at all levels. The diurnal cycle of DmSS peak wind speeds also showed over-estimates throughout the 24-hour day, with greater over-estimates during the day-time hours.

A statistical model of an idealized phased-array Doppler profiler was developed to aid in the interpretation of DmSS comparisons with wind tower data. The model predicted accurate profiler performance for average wind speeds, consistent with the comparative study of DmSS and wind tower data. The model also predicted that peak wind speeds from the profiler would be over-estimated due to a combination of an under-specification of vertical velocity variations by the phased array scanning sequence and the mathematical form of retrieval algorithms required for estimating peak wind speeds. In addition, the model predicted that the magnitude of the over-estimate in peak wind speeds would be positively correlated with the magnitude of variability in the vertical velocity, which maximizes during the day-time hours. The three predicted characteristics listed above were observed in the comparison of DmSS and wind tower data.

Table of Contents

List of Figures

List of Tables

1. Introduction

The MiniSODAR™ (AeroVironment, Inc. 2001) is a meteorological instrument that uses Doppler and SOund Detection-And-Ranging (SODAR) technologies to obtain vertical profiles of wind speed and direction. The Boeing Company installed this Doppler miniSODAR™ System (hereafter DmSS) near Space Launch Complex 37 (SLC-37) in mid-2002 as a substitute for a tall wind tower. Boeing plans to use the DmSS to monitor launch pad winds for the new Evolved Expendable Launch Vehicles during ground operations and to evaluate user Launch Commit Criteria (LCC) during launch operations. Observations of peak winds are an essential element of the user LCC. In order to make critical GO/NO GO launch decisions, Launch Weather Officers (LWOs) and forecasters from the 45th Weather Squadron (45 WS) need to know the quality and reliability of DmSS data, especially as it applies to peak wind speeds. The Applied Meteorology Unit (AMU) compared average and peak wind speed data from the SLC-37 DmSS with average and peak wind speed data from nearby wind towers for the time period from August 2002 to July 2003. Results of the comparison are reported in detail below.

Remote sensing systems that combine Doppler and SODAR technologies for wind profiling have been successfully demonstrated since the early-1970s (Hall et al. 1975), and AeroVironment, Inc. has been a leading developer of Doppler/SODAR wind profiling systems for the past two decades. The DmSS has been commercially available for more than a decade and was rigorously tested in 1995 with two other acoustic wind profilers at the Boulder Atmospheric Observatory (BOA). The BOA is a research facility operated by the National Atmospheric and Oceanic Administration (NOAA) for studies of the planetary boundary layer and testing of various atmospheric sensors. Based on a 3-week field trial with 15-minute average wind speed and direction comparisons to a calibrated wind tower, the NOAA report concluded that the acoustic wind profiling technology was mature and should be used for routine monitoring applications (Crescenti 1999). The primary caveat was finding a suitable site for the acoustic instrument, to minimize effects of external acoustic noise sources and obstacles that may be potential reflectors of acoustic signals. More recently, a DmSS was successfully operated aboard a research vessel to measure average wind speed and direction profiles at sea, with temporal averaging over a minimum time period of 15-minutes (Barthelmie et al. 2003).

However, the AMU is not aware of any previous evaluation of DmSS peak wind data, particularly as it would apply to the operational environment associated with ground and space launch activities.

2. Instrument and Data Descriptions

The DmSS is a phased array system with 32 speaker elements that are used to form an electronically-steered beam. The beam can be pointed in 3 directions, 1 vertical and 2 oblique. The oblique beam positions are designed to obtain information on the horizontal wind components and are in orthogonal planes to optimize the accuracy of wind speed and direction measurements. However, they are tilted only 16 degrees off the vertical in order to avoid potential contamination by echoes from ground targets. As a result, each oblique beam measures a trigonometrically weighted sum of the vertical and horizontal wind velocities along the beam axis. This configuration is successful because the vertical wind speed is usually much less than the horizontal wind speed. Nevertheless, algorithms for retrieving horizontal wind speed and direction information with high temporal resolution must use the vertical wind velocity information from the vertical beam to correct the observations from the oblique beams.

The DmSS cycles through the 3 beam positions every 2.58 seconds, providing a maximum of 24 data triplets every minute for retrieving speeds and directions of the average and peak horizontal winds. The DmSS is configured to provide wind retrievals at 23 height levels from 49.2 to 410.1 ft (15 to 125 m) with a vertical resolution of 16.4 ft (5 m). The combination of vertical and angular resolutions of the 3 beams (~5° each) indicate that the DmSS provides wind speed and direction data over a volume of atmosphere, referred to as a range gate, approximately 16.4 ft deep and 9 ft in diameter at an altitude of 100 ft. At the maximum altitude of 410.1 ft the range gate is 36 ft in diameter.

The temporal resolution of DmSS data can be varied from 30-seconds to 1-hour depending on the application. For most of the period of this study the DmSS has been configured to provide 1-minute data. The 1-minute temporal resolution is consistent with the real-time displays of data from the wind tower network on Cape Canaveral Air Force Station (CCAFS) and Kennedy Space Center (KSC). The DmSS has occasionally been configured to provide retrievals every 30 seconds to provide more rapid updates during operations.

Wind sensors on the towers closest to SLC-37 are propeller-type anemometers with a fuselage and wind vane (R. M. Young Model 05305-18 Wind Monitor-AQ sensors). These are high performance sensors designed to support air quality type measurements. The AMU obtained the 5-minute tower data from Computer Sciences Raytheon (CSR; Mr. Paul Wahner). The data archive includes average wind speed and wind direction, and peak wind speed and direction for 5-minute intervals beginning at the top of each hour. The data processed by CSR were comprised of 300 observations at 1-second intervals for each 5-minute time block.

2.1. Sensor Locations

Figure 1 shows the locations of the DmSS and the nearest wind towers. The tall wind tower (≥ 204 ft) that is nearest to SLC-37 is Tower 0006 at 0.95 n mi. Tower 0006 has wind sensors at 12, 54, 162 and 204 ft. Tower 0108 with a maximum height of 54 ft is closer, at 0.6 n mi, to the DmSS than Tower 0006, as shown in Figure 1, and will also be used in the comparison study. Tower 0108 has wind sensors at 12 and 54 ft. Mr. Wheeler began collecting data from these towers and the DmSS in June 2002.

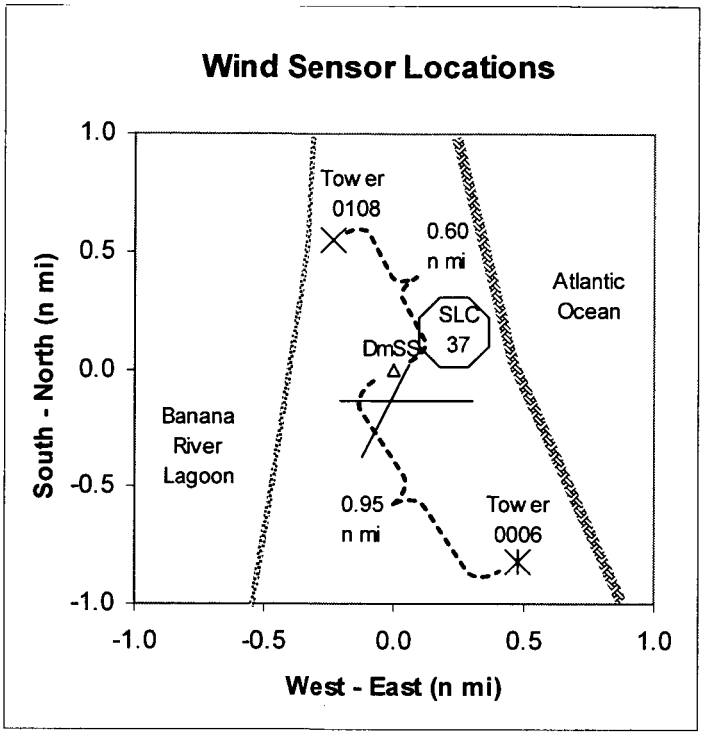

Figure 1. Locations of Towers 0006, 0108 and the DmSS, with approximate geographic features. The intersecting solid lines near the DmSS site indicate nearby roads.

2.2. Siting Issues

Figure 2 shows the DmSS where it was installed by Boeing on a concrete pad approximately 0.25 nm I SW of SLC-37. The view direction in the photograph is toward the SW. General guidelines from the World Meteorological Organization (WMO) for wind sensor sites are to place them at a distance at least ten times the height of the nearest obstruction (WMO 1983) to avoid local distortions of wind flow around the obstruction. It appears that the wind field at the present DmSS site could be influenced by the pictured building, approximately 40 ft away, especially when the wind blows from the SW quadrant.

An additional factor that could affect data quality would be traffic along the 2-lane road that runs parallel to the front of the building, about 60 ft to the left of the location in Figure 2. It is possible that the DmSS signal would be influenced by acoustic noise or reflected sound waves from vehicles traveling along the road, which has a posted speed limit of 35 mph, or 30.4 kts. One possible solution for minimizing such effects would be to add acoustic baffles to the DmSS. A routine maintenance schedule for the DmSS is also advised by the manufacturer to assure that it remains fully operational (AeroVironment, Inc. 2001). The loss of a speaker element would compromise the beam form, increasing the probability of unwanted contamination of acoustic signals and erroneous wind retrievals.

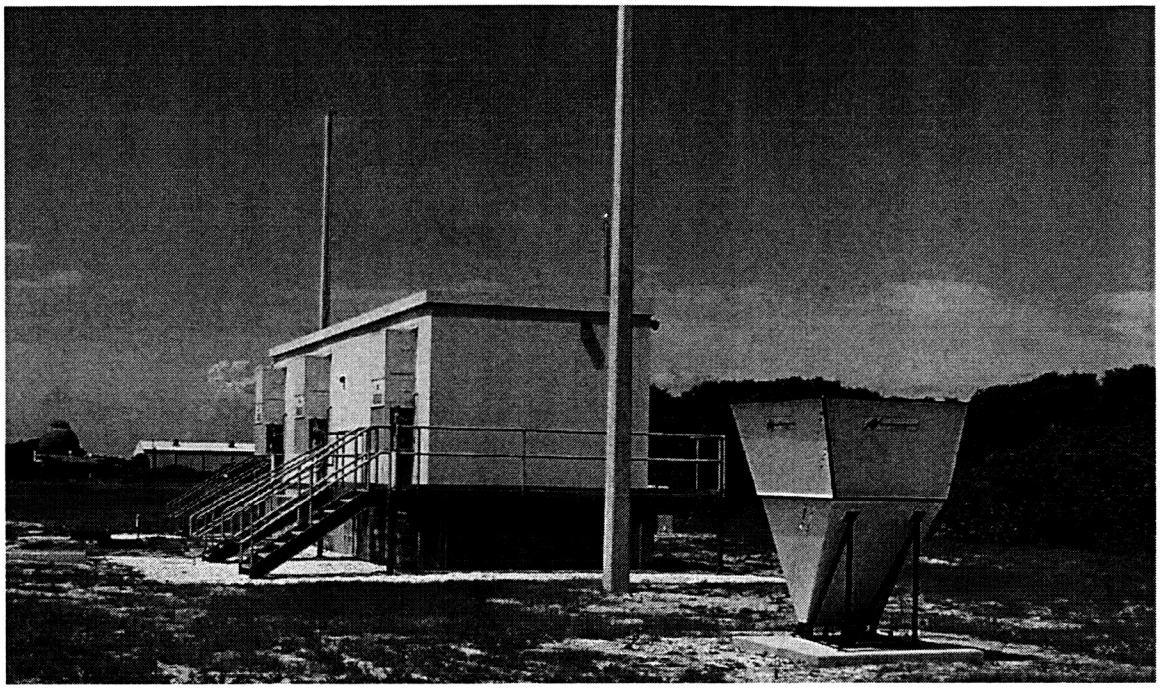

Figure 2. Photograph of DmSS site and nearby building. The DmSS and building are separated by about 40 ft. A 2-lane road runs parallel to the front of the building approximately 60 ft to the left. The DmSS site includes a sonic anemometer on a 33 ft (10 m) pole that is behind the building and partially obscured from view by the pole in the foreground. Sonic anemometer data are integrated into the DmSS data stream.

The distance between the DmSS and the nearest wind towers influenced the nature of the comparisons and conclusions that have been drawn from analyses of the data. Turbulent variations of wind speed and direction can result in differences between sensor readings, even for instruments with no errors, due to the physical separation of the sensors. The difference in sensor readings is expected to increase as the distance between the sensors increases. However, differences can be expected to decrease as the time averaging of the data increases. The theoretical difference, in percent squared, for a comparison under ideal conditions can be modeled by the following equation (Crescenti 1997):

$$\varepsilon^2 = \frac{2}{T}\frac{\sigma_U^2}{U^2}\int_0^\infty R(t)\,dt \qquad (1)$$

where T is the averaging time-scale for the data, U is the prevailing wind speed along the line between the sensors, σ_u is the standard deviation of wind speed and R(t) is the autocorrelation function of the wind speed. The integral can be represented by a second time-scale equal to d/U, where d is the separation distance. The ratio σ_u/U has been found to be approximately 0.224 in previous studies (Wyngaard 1973). Note that the theoretical difference decreases as the averaging time T increases.

Figure 3a shows the expected difference as a function of separation distance for a wind speed of 10 kt and data averaging times (T in Equation 1) of 5, 10, 20 and 40 minutes. For example, at a separation distance of 0.6 n mi with an average wind speed of 10 kt (U in Equation 1), an averaging time of 40 minutes would be expected to result in comparison differences of +/- 1 kt (10%). A 5-minute averaging time under the same conditions would result in comparison differences of +/- 2.7 kts (27%). Figure 3b shows that the expected differences for a wind speed of 20 kt are less than those for a wind speed of 10 kt for all comparable averaging times.

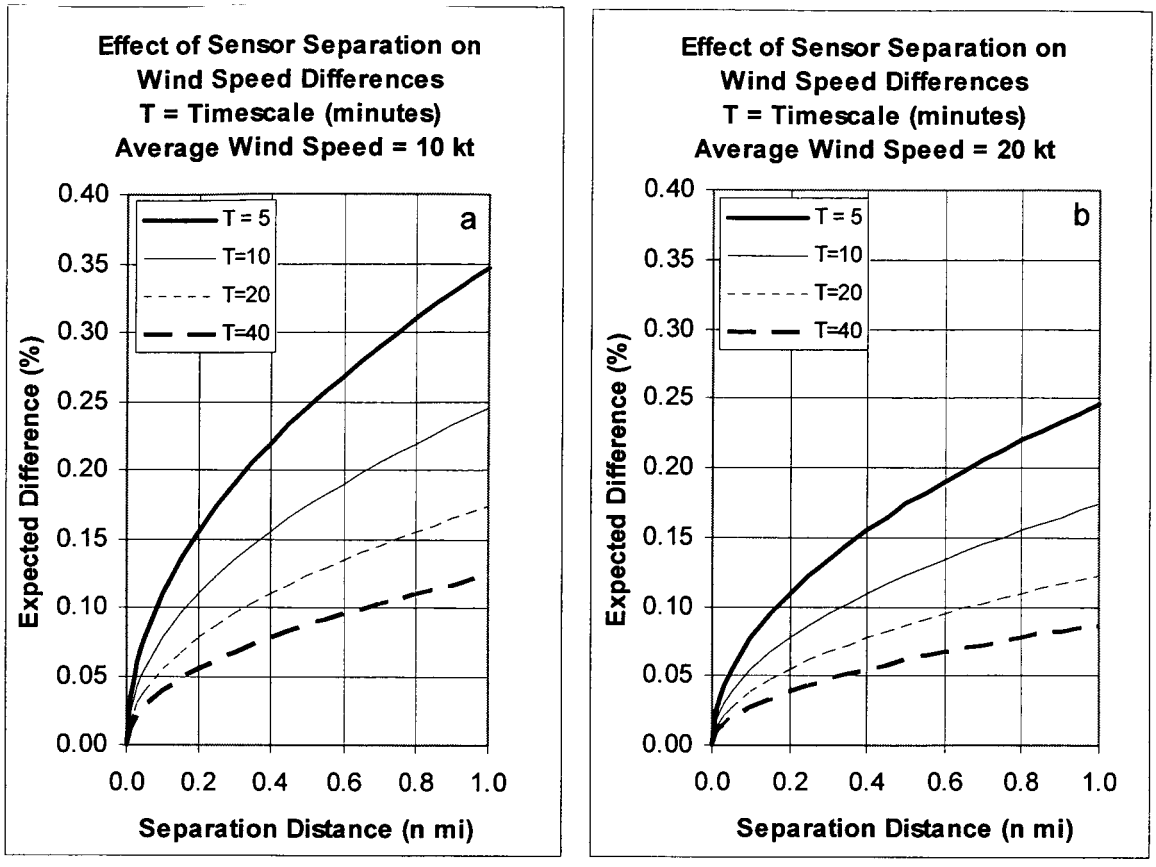

Figure 3. Expected differences as a function of separation distance for wind speed comparisons under ideal conditions. Curves are for timescales of 5, 10, 20 and 40 minutes and for average wind speeds of 10 kt (a) and 20 kt (b). The curves are based on the statistical model expressed in Equation 1.

2.3. DmSS Data Structure

The DmSS data are recorded on a personal computer (PC) system in the Range Weather Operations (RWO) facility within the Range Operations Control Center. The AMU obtained permission from the 45 WS and Boeing to download DmSS data from the RWO PC on a non-interference basis. The AMU archive contains 14 months of DmSS data covering the period from June 2002 to July 2003.

The RWO PC records a block of DmSS data every minute with date/time information, system configuration parameters and wind information at 24 levels. The highest 23 levels are DMSS data and the lowest level (33 ft) is from the sonic anemometer. The wind data includes wind speed and direction information when available and a missing data code otherwise. Reasons for DmSS missing data include a low signal-to-noise ratio (SNR) and precipitation. Numerous measures of DmSS performance such as signal intensity and signal-to-noise ratio are also reported. Table 1 lists the 20 fields that are routinely recorded.

Table 1. DmSS parameters recorded every minute.	
Number	Parameter
1	Height (m)
2	Average Wind Speed (m/s)
3	Average Wind Direction (degrees)
4	W-component (Average Speed; m/s)
5	W-component (Standard Deviation; m/s)
6	W-component (Signal Intensity)
7	Wind Gust Speed (m/s)
8	Wind Gust Direction (degrees)
9	U-component (Average Speed; m/s)
10	U-component (Standard Deviation; m/s)
11	U-component (Number of Samples)
12	U-component (Signal Intensity)
13	U-component (Signal-to-Noise Ratio)
14	V-component (Average Speed; m/s)
15	V-component (Standard Deviation; m/s)
16	V-component (Number of Samples)
17	V-component (Signal Intensity)
18	V-Component (Signal-to-Noise Ratio)
19	W-Component (Number of Samples)
20	W-component (Signal-to-Noise Ratio)

3. Comparisons with Wind Tower Data

The vertical profiles and diurnal cycles of data availability, average wind speed/direction, and peak speed from each instrument were created for the comparison. Direct comparisons of the average and peak wind parameters were based on simultaneous 5-minute averages of DmSS and wind tower data. Over-all data availability for the DmSS was based on 1-minute observations, whereas the wind tower availability was based on 5-minute data. The vertical profiles and diurnal cycles of these characteristics are documented in this section for representative time periods to illustrate various aspects of DmSS performance during the 1-year evaluation.

3.1. Data Availability

In this study, a reported wind speed and wind direction was defined as available data for the DmSS and wind tower data streams. Missing data blocks from the DmSS and wind towers were interpreted as missing data, except for scheduled instrument or communications outages. Missing data codes within the DmSS data block were interpreted to indicate that the data was unavailable. Combinations of atmospheric conditions and/or instrument function can result in DmSS missing data codes. For example, a SNR that is too low for reliable wind retrieval can be caused by background noise, atmospheric attenuation of the acoustic signal, weak atmospheric backscattering of the acoustic signal, degraded performance of the acoustic transmitter/receiver array, or combinations of all such relevant factors. The vendor recommends a routine schedule of preventative maintenance on the DmSS to assure continued good performance and reliable operation (AeroVironment, Inc. 2001). Data availability can be expected to vary as a function of the operational status of the DmSS, the background noise level, and atmospheric conditions.

The availability of DmSS data showed a considerable dependence on height, the diurnal cycle, the presence of precipitation, and on the operational status of the instrument. Only graphs of DmSS data availability are presented in this section because the availability of wind tower data during the study was consistently 99.7% or higher, averaging approximately 1 missing 5 minute block per day or less with no dependence on height, the diurnal cycle or precipitation.

Vertical Profile

Figure 4 shows the vertical profile of DmSS data availability (solid line) for an 18 day period from October 10-28, excluding the 14th, due to a scheduled outage. The general decreasing trend of data availability with height is characteristic of acoustic wind profiling systems (Crescenti 1997) as echo returns become weaker and the SNR decreases with increasing distance from the speaker array. Data availability at the 98 ft level monitored by the Delta LWO during operations was 99.2%. On the morning of 9 October 2002 preventative maintenance had been performed on the DmSS by the vendor. Several speaker elements in the phased array were replaced. Figure 4 also shows a comparison of DmSS data availability for the first 8 days of the month before the maintenance (dashed line). The fraction of missing observations at the 98-ft decreased from 3.9% to 0.8% after maintenance.

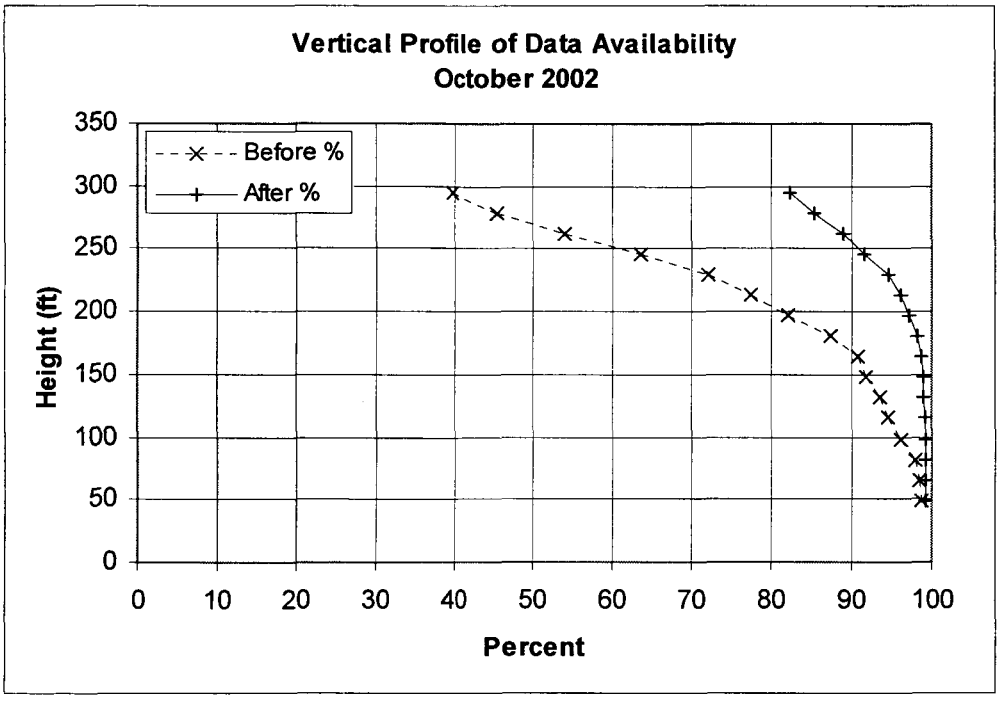

Figure 4. Vertical profiles of data availability from the DmSS before and after maintenance on 9 October 2002. The minimum wind retrieval height is 49.2 ft (15 m).

Figure 5 shows vertical profiles of data availability after preventative maintenance was performed in early June 2003. Overall data availability was slightly less than that shown for the post-maintenance October example (Fig. 4) for two reasons. 1) The increased temperature and relative humidity in June resulted in a greater attenuation of acoustic signals (Crescenti 1998) and 2) the June data were filtered by eliminating retrievals where the standard deviation of U or V (see Table 1) was greater than 2 kts. The latter criterion was recommended by the vendor in January 2003 to eliminate high speed outliers not representative of meteorological conditions.

Figure 5 also illustrates effects of rain on data availability. The DmSS has an automatic algorithm that identifies rainfall and reports the missing data code. During the 15-day period from 16 to 30 June data availability below 100 ft averaged 92% and the average rainfall recorded by the KSC/CCAFS rain gauge network was 4.01 in. During the 6-day interval from 23 to 28 June data availability below 100' averaged 97% and the average rainfall was only 0.08 in.

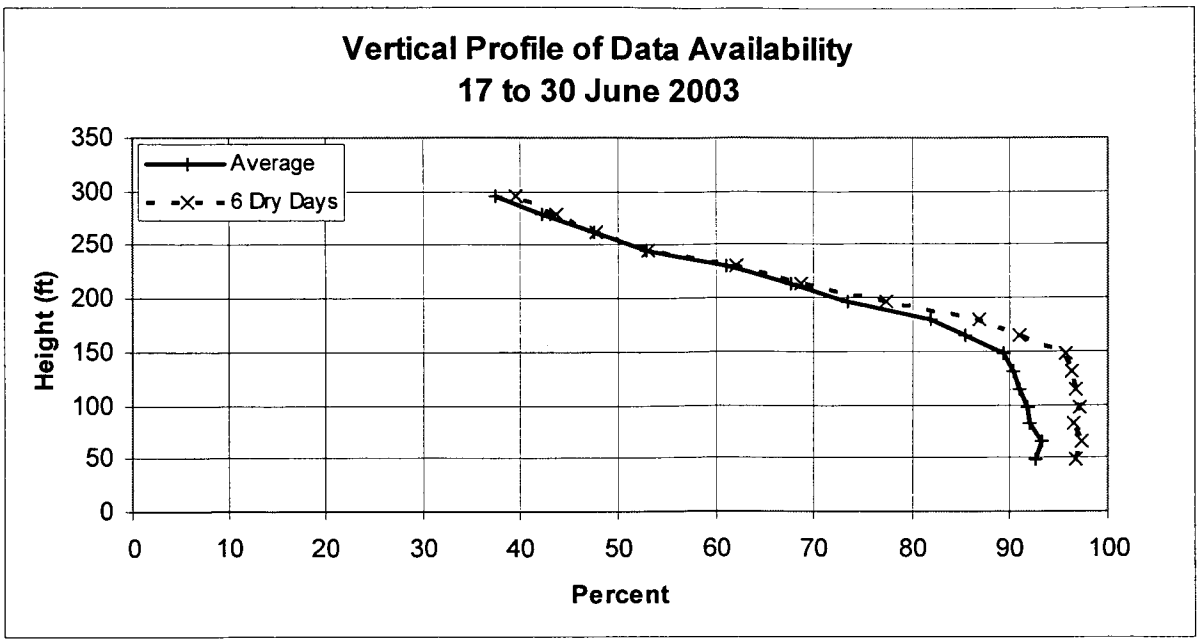

Figure 5. Vertical profiles of DMSS data availability for 14 days from 17 - 30 June 2003 (solid) and for 6 days from 23 - 28 June 2003 (dashed). The latter period was a dry interval in which an average 0.08 in of rain was recorded by the KSC/CCAFS rain gauge network, contrasting with an average 4.01 in recorded during the full period.

Diurnal Cycle

The daily cycle of surface heating and cooling, combined with turbulent mixing in the atmospheric boundary layer produces small scale temperature variations in the air. These variations are the source of acoustic backscattering relied upon by acoustic wind profiling techniques. DmSS echo strength is dependent on the amplitude of these small scale temperature variations (AeroVironment, Inc. 2001). As a result, data availability can also show a diurnal cycle.

Figure 6 shows the diurnal cycle of DmSS average data availability at selected heights during the 6-day dry interval in late June 2003. There are noticeable minima at 1000 and 2200 UTC or 0600 and 1800 local time, around sunrise and just before sunset. Just after sunrise the cool surface and lower atmosphere begin to warm up until a near iso-thermal layer is formed. The effect of this layer is to minimize the amplitude of small scale atmospheric temperature variations, resulting in weaker acoustic echoes, a smaller signal-to-noise ratio, and a reduction in data availability. As the surface and lower atmosphere heat up during the day a vertical temperature gradient is established increasing the amplitude of small scale temperature variations resulting in stronger acoustic echoes. Surface solar heating during the day also produces buoyant thermal plumes, enhancing small scale temperature variations and increasing data availability. As the sun sets, surface cooling results in a near iso-thermal layer and reduced data availability (near 2200 UTC). During the night-time hours a temperature inversion typically exists with cooler air near the surface and warmer air aloft. This reverse temperature gradient also results in small scale temperature variations due to mechanically produced turbulence produced by surface roughness and vertical shear in the wind speed profile. Reductions in data availability throughout the diurnal cycle increase monotonically with height. The large decrease in data availability above 98 ft during the night-time hours is consistent with previous studies of Doppler/SODAR profilers (Crescenti 1999).

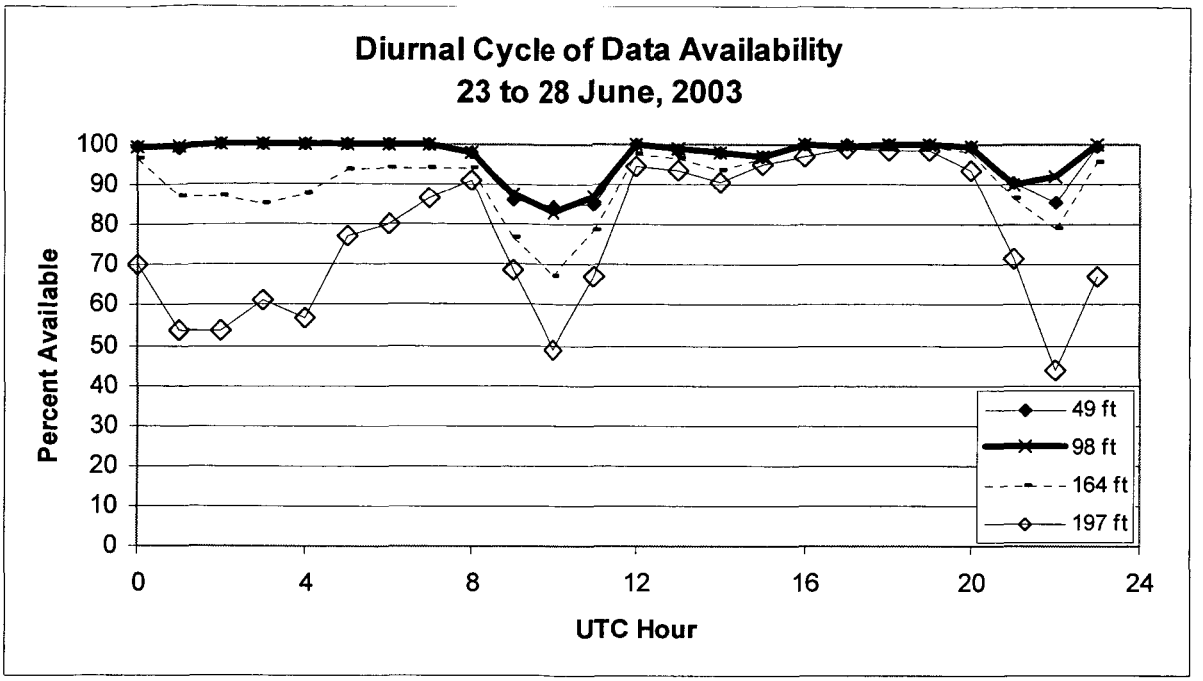

Figure 6. Diurnal cycle of data availability during the 6-day interval from 23 to 28 June 2003. Data from 4 heights are shown: 49 ft, 98 ft, 164 ft and 197 ft. Sunrise was at ~1025 UTC. Sunset was at ~0025 UTC.

Figure 7 shows the diurnal cycle of DmSS average data availability during the period from 17 - 30 June 2003. Evidence of minima at 1000 and 2200 UTC are seen, as in Figure 6, in addition to reduced data during the daytime and early evening hours due to rainfall.

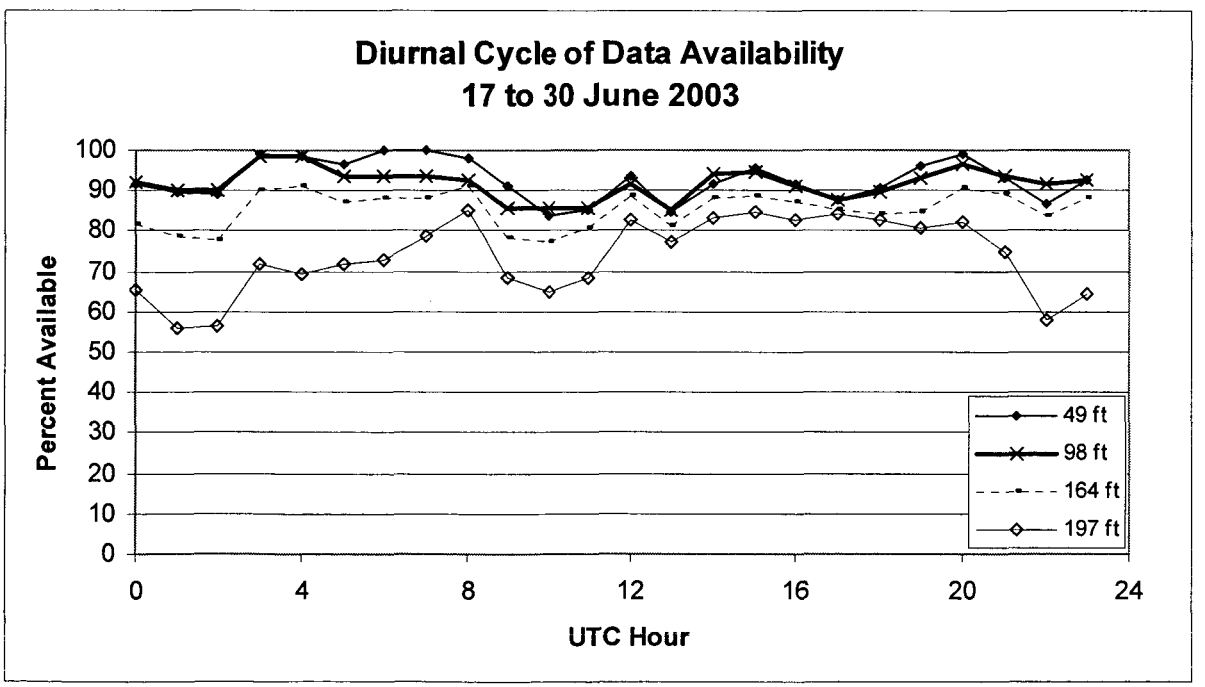

Figure 7. Same as Fig. 6 but for 14-day period from 17 - 30 June 2003.

3.2. Average Wind

The following example of time-coincident DmSS and tower data is representative of the type of wind direction comparison that can be made for evaluating DmSS performance given the distances between instruments shown in Figure 1. Figure 8 shows a 6-hour time series from 1200 – 1800 UTC on 28 August 2002 of 5-minute average wind direction from the DmSS and Towers 0006 and 0108. Data from the 54 ft level on the towers and the nearest level on the DmSS (49.2 ft or 15m) were used. The passage of a sea breeze was clearly evident around 1630 UTC. Wind directions shifted from SW to ESE at Tower 0006 first, at the DmSS site next, and then at Tower 0108. This delayed timing is consistent with a sea breeze moving inland from the east-southeast toward the west-northwest.

Figure 8 also shows a longer term trend of wind direction change before the sea breeze passage, from 1200 to 16000 UTC. The long-term trend was detected by the DmSS and both wind towers. Superposed on the long-term trend are short-term directional variations from all three sensors. The pattern of short-term variations in wind direction was too complex to interpret as a simple propagating phenomenon. The complexity and lack of coherence at short time-scales is typical of the turbulent wind field near the earth's surface.

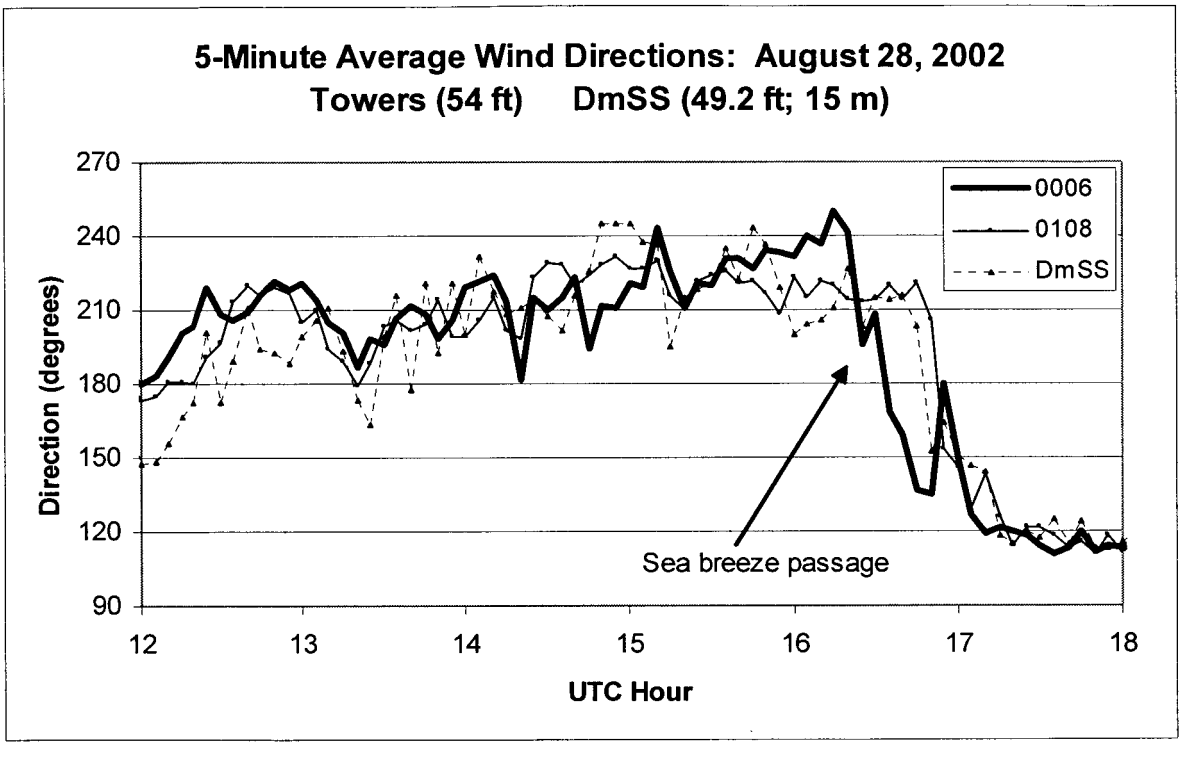

Figure 8. A 6-hour time series of wind direction from 54 ft on Towers 0006 and 0108, and the 49.2 ft (15 m) from the DmSS. A sea breeze passage is indicated around 1630 UTC.

Figure 9 shows a representative example of 5-minute average wind speed data from Tower 0006 and the DmSS. The time series shows data at 162 ft from Tower 0006 and at 164 ft from the DmSS for the 24-hour interval (UTC) on 10 March 2003. Wind speeds varied from near calm to 15 kts throughout the course of the UTC day. Both sensors showed the same overall trends and the daily average wind speeds from each instrument were within 4% (9.31 versus 8.94 kts) of each other. However, short-term variations were poorly correlated as expected, because of the distance between the sensors. The root-mean-square difference between the sensors was 1.82 kts, or 20% of the overall average. This average difference was within a range that could be expected due to short-term turbulent fluctuations in the atmospheric boundary layer that are incoherent over the distance separating the two sensors (see Fig. 3). Therefore, the observed differences were not large enough to be considered statistically significant for this example.

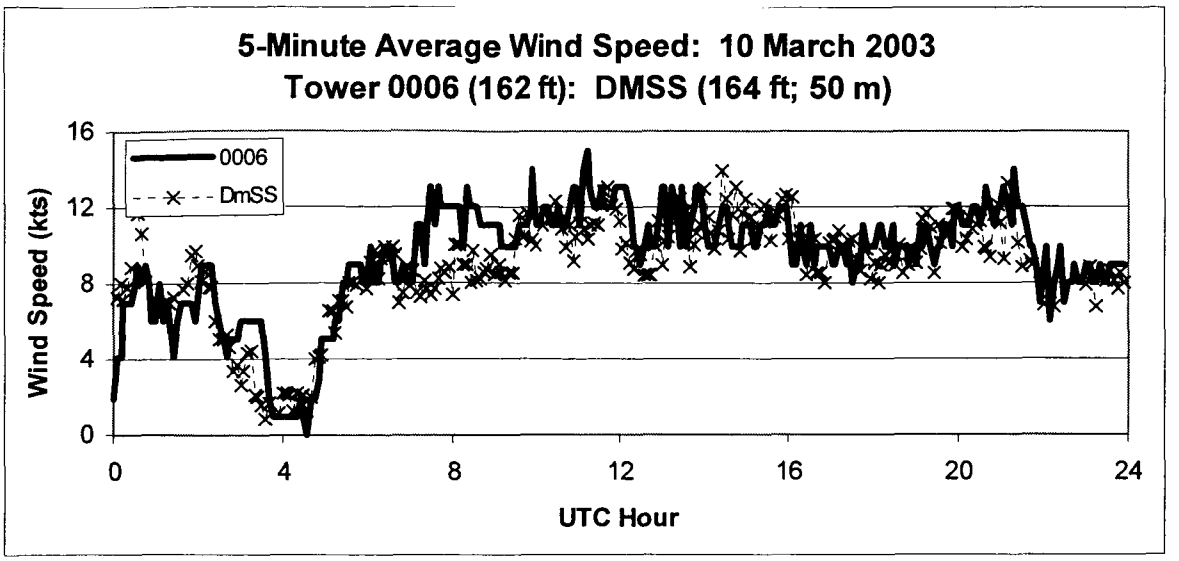

Figure 9. A 24-hour time series on 10 March 2003 of 5-minute average wind speeds at 162 ft on Tower 0006 and the 164 ft level of the DmSS. The average wind speeds were 9.31 kts (tower) and 8.94 kts (DmSS).

Vertical Profile

Figure 10 shows a vertical profile of the mean 5-minute average wind speeds from Towers 0006 and 0108, the DmSS and the sonic anemometer for the DmSS post-maintenance period from 17 - 30 June 2003. There is good agreement between the wind towers and the DmSS. This result is consistent with the daily time series for an earlier period shown in Figure 9. It is also consistent with previous studies of DmSS performance in measuring average wind conditions using this commercially available instrument (Crescenti 1999; Barthelmie et al. 2003).

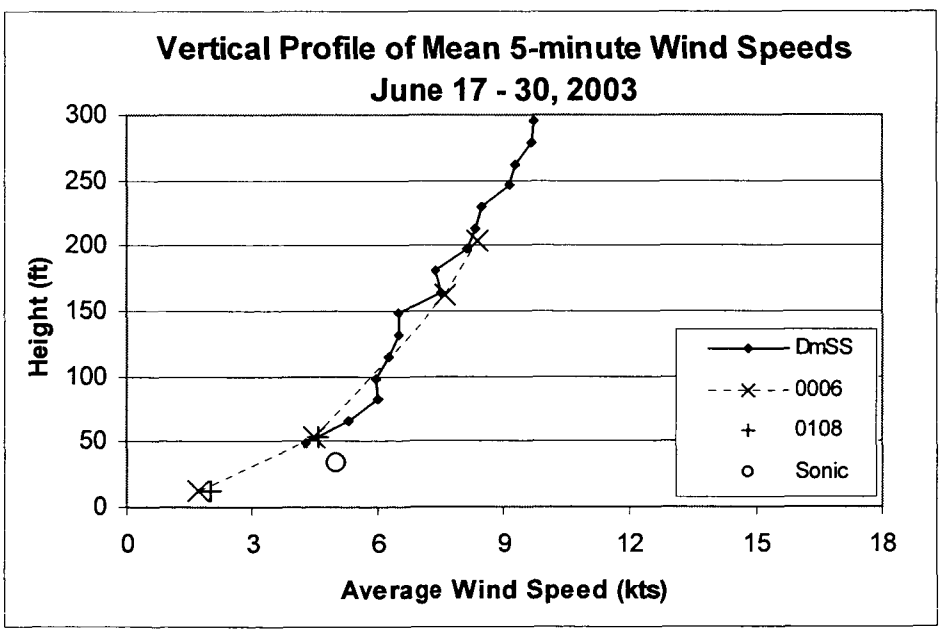

Figure 10. Vertical profiles of mean 5-minute average wind speed during 17 - 30 June 2003 from the DmSS and Towers 0006 and 0108. The open circle indicates data from the sonic anemometer at the DmSS site.

Diurnal Cycle

Figure 11 shows the diurnal cycle of mean 5-minute average wind speed from the DmSS and Tower 0006 for the 14 day period 17 - 30 June 2003. There was generally good agreement with slightly lower speeds observed by the DmSS during the nighttime hours (0000 - 1100 UTC) and slightly higher speeds during the daytime hours. There was insufficient information available to determine if the small systematic differences in wind speed were due to instrument performance or real differences in wind conditions at the two sites over the course of the diurnal cycle.

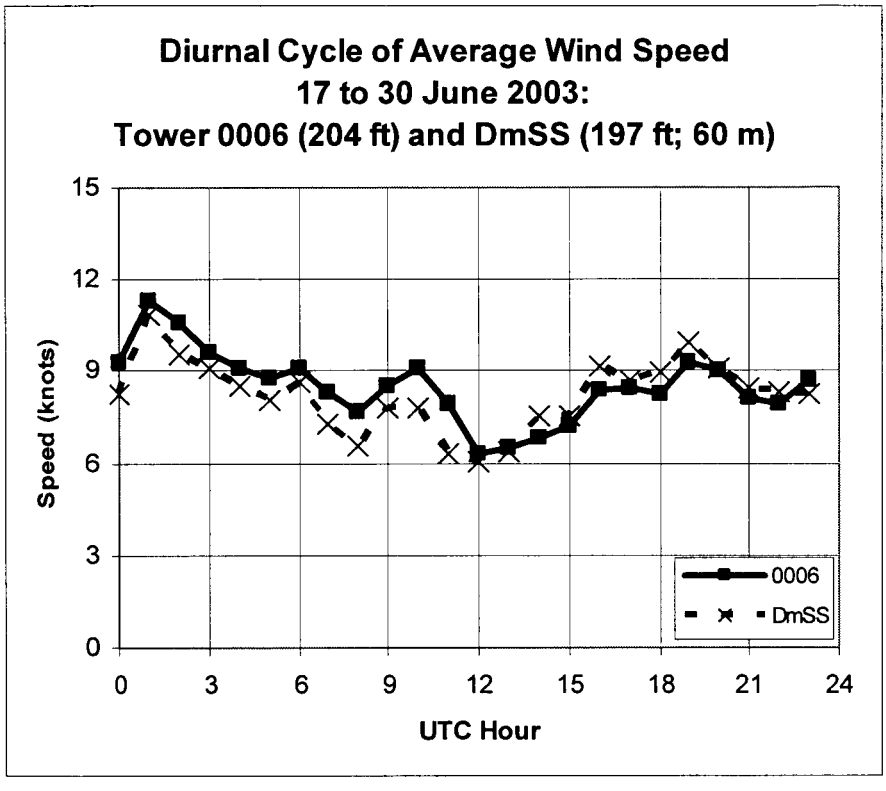

Figure 11. Diurnal cycle of the mean 5-minute average wind speed at 204 ft on Tower 0006 and at 197 ft from the DmSS.

3.3. Peak Wind

Figure 12 shows a representative example of 5-minute peak wind speed data at 162 ft from Tower 0006 and at 164 ft from the DmSS. The time series is for the 24-hour UTC interval on 10 March 2003. Peak wind speeds from the tower varied from near calm to 20 kts throughout the UTC day. However, peak wind speeds from the DmSS varied from 5 kts to > 25 kts. Both sensors showed the same overall trends, but the DmSS peak wind speeds were higher than those from the tower, except for about 1 hour near 0800 UTC. The daily average of peak wind speeds reveal that the DmSS was ~25% higher than the tower (15.7 versus 12.6 kts). It is important to note that the average wind speed for the same time period (see Fig. 9) showed good agreement, despite the apparent bias in peak wind speeds shown in Figure 12.

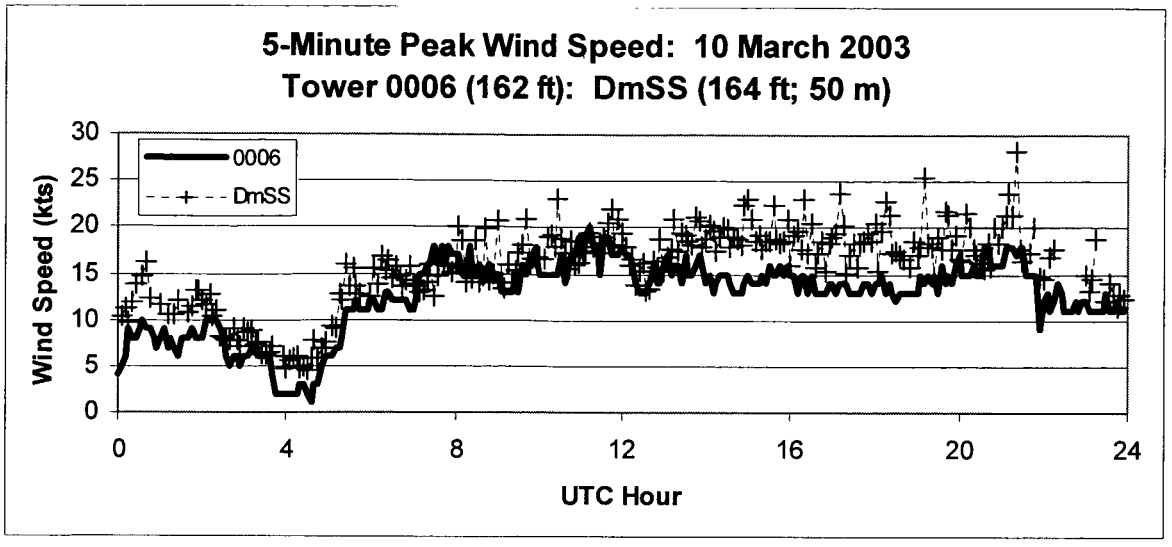

Figure 12. A 24-hour time series of peak wind speeds at 162 ft on Tower 0006 and 164 ft from the DmSS. The daily average of the peak wind speeds were 12.6 kts (tower) and 15.7 kts (DmSS).

Vertical Profile

Figure 13 shows a vertical profile of average peak wind speed for Towers 0006 and 0108 and the DmSS during the post-maintenance 14 day period from 17 - 30 June 2003. The average DmSS peak wind speed was greater than the average peak wind speed from the towers at all available levels. The bias ranges from 15% at 50 ft to 25% at 200 ft. This result is consistent with the bias seen in the time series for the earlier period shown in Figure 12. It is also useful to contrast Figure 12 with Figure 10 which shows a good agreement between the DmSS and wind towers with respect to the vertical profile of average wind speeds. This contrast suggests an inconsistency in the way the DmSS determines average and peak wind speeds.

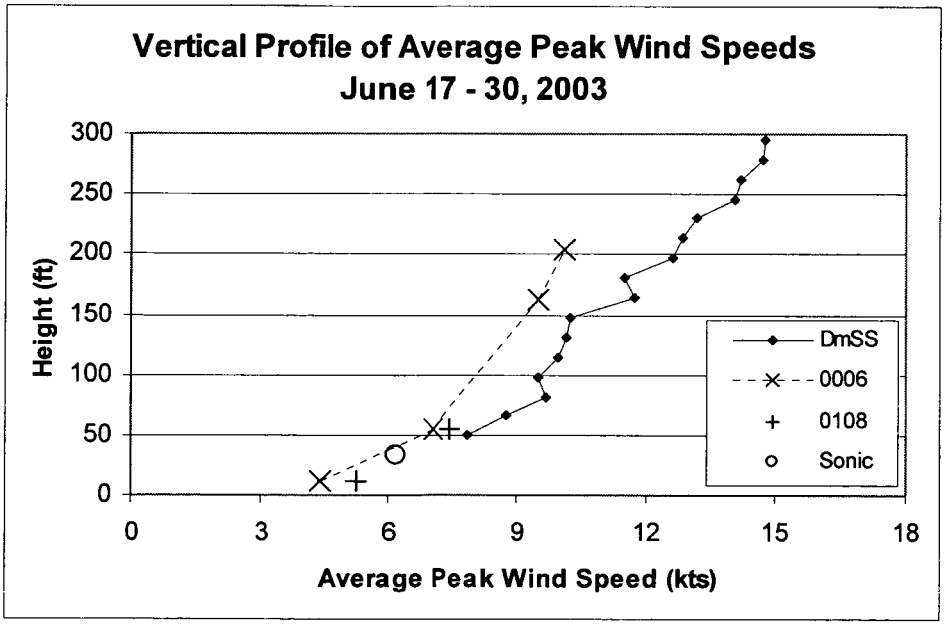

Figure 13. Vertical profiles of the average peak wind speed for the time period from 17 to 30 June 2003 from the DmSS and wind towers 0006 and 0108. The open circle indicates data from the sonic anemometer at the DmSS site.

Diurnal Cycle

Figure 14 shows the diurnal cycle of the average peak wind speeds from the DmSS and Tower 0006 for the 14 day period from 17 - 30 June 2003. There was a systematic bias of higher average peak speeds observed by the DmSS during all hours of the day. The average DmSS peak speeds were ~ 20% higher than the tower speeds during the night-time hours and increased to as much as 50% higher during the day-time hours.

Figure 14 also shows the standard deviation of vertical wind speed (σ_W) from the vertical beam of the DmSS, multiplied by a factor of 10. Note that σ_W increased from about 0.5 kts during the night-time hours (0000 to 1200 UTC) to greater than 1 kt during the day-time hours. The day-time increase in σ_W was consistent with the influence of thermal plumes produced by day-time heating of the surface. Theoretical considerations will be presented in Section 4 that indicate peak wind speed retrievals from a phased array Doppler profiler are susceptible to a high bias, similar to that seen in Figures 12, 13, and 14, that the bias is proportional to the standard deviation of the vertical air velocity.

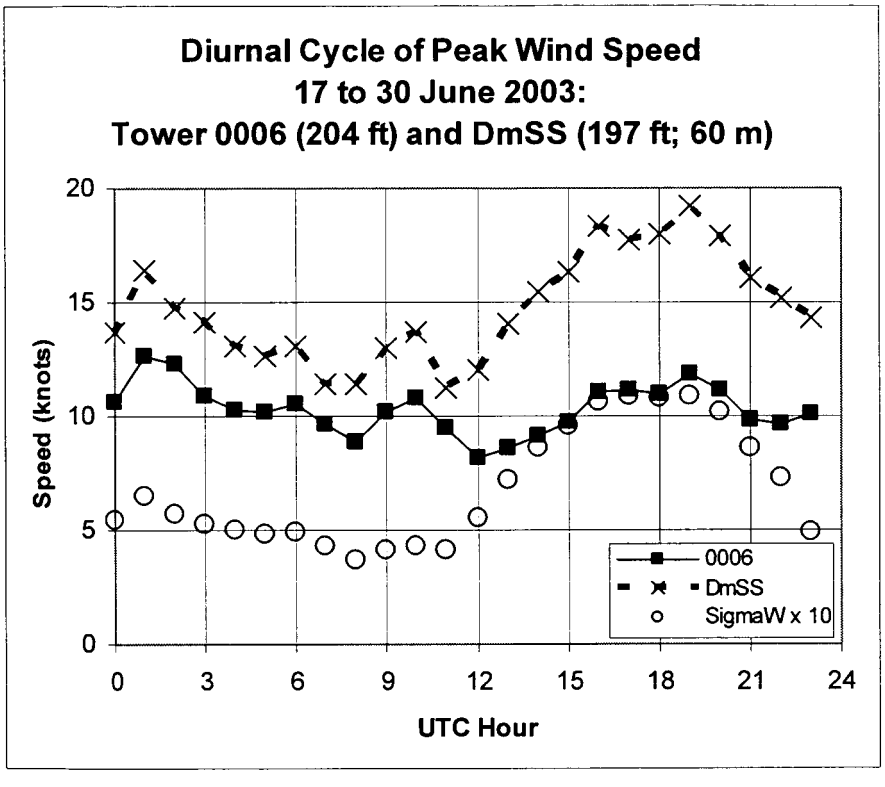

Figure 14. Diurnal cycle of the average peak wind speed at 204 ft on Tower 0006 and at 197 ft from the DmSS. The standard deviation in vertical wind speed, multiplied by a factor of 10, is also shown (O).

4. Theoretical Considerations for Peak Speed High Bias

The following mathematical description of an idealized, phased-array Doppler wind profiler is intended to represent, in the simplest terms, how the true horizontal and vertical wind velocity components affect measurements from the oblique and vertical beams of a system configured like the DmSS. A physically-based algorithm is then presented that utilizes the vertical and oblique beam measurements to retrieve horizontal wind speed. The retrieved wind speed is shown to be susceptible to an error that has its roots in an under-sampling of the vertical wind velocity over the profiler beams. A statistical model is used to simulate realistically varying horizontal and vertical wind speeds, the resulting profiler observations, and retrieved wind speeds. This statistical modeling approach quantifies three important characteristics that are consistent with the comparative analysis of DmSS and wind tower data shown in Section 3: 1) The average retrieved wind speed was unbiased, 2) The average retrieved peak wind speed was positively biased, and 3) The model also indicates that the magnitude of the bias depends on the standard deviation of the vertical velocity. Although the actual DmSS retrieval algorithms are proprietary, the idealized statistical modeling approach warrants consideration as a valid method for understanding the nature and magnitude of the DmSS and wind tower comparisons presented in this study.

4.1. Idealized Phased-Array Doppler Wind Profiler

Consider an idealized, phased-array Doppler profiler that measures the radial velocity along each of two beams, b_1 and b_2, as in Figure 15. The b_1-beam is vertically oriented with respect to the local horizontal plane. The b_2-beam is oriented at an angle Θ from the vertical in order to measure the horizontal (u) component of the wind.

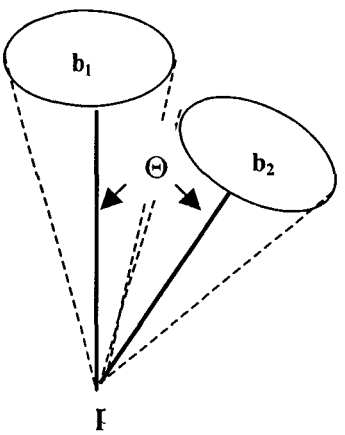

Figure 15. Schematic of an idealized 2-axis phased array Doppler wind profiler system.

The profiler obtains doublets of radial velocity, $V_1(R_1, t_1)$ and $V_2(R_2, t_2)$, as the acoustic beam is electronically switched from position b_1 at time t_1 to position b_2 at time t_2. The symbols R_1 and R_2 denote ranges from point p in Figure 15, the location of the instrument. Note that the b_2-beam is tilted at only a small angle away from the vertical in order to avoid side-lobe contamination from ground targets with zero-Doppler shift. As a result, $V_2(R_2, t_2)$ can be significantly affected by the vertical wind component. The condition $R_1 = R_2 \cdot \text{Cos}(\Theta)$ is required to obtain radial velocities at the same altitude, $H = R_1$, above the local horizontal plane. The following notation was developed by assuming this condition was met and by dropping the notation for height and range.

Equations for a Uniform Wind Field

Under idealized conditions of temporal and spatial uniformity in the wind field, the idealized profiler observations are described by the following equations (Peterson 1988):

$$\mathbf{V_1 = w} \tag{1}$$

$$\mathbf{V_2 = u \cdot \sin(\Theta) + w \cdot \cos(\Theta)} \tag{2}$$

where **w** is the vertical component of the wind velocity and **u** is the horizontal component of the wind velocity.

Equation 2 can be directly solved for the **u** component of the wind as follows:

$$\mathbf{u} = \mathbf{V}_2 \cdot \sec(\Theta) - \mathbf{w} \cdot \cot(\Theta) \tag{3}$$

There are three important points to note from Equations 1-3:

1. Equation 1 shows that the vertical velocity is obtained from $\mathbf{V}_1$, the radial velocity measured by the b_1-beam.
2. The vertical velocity, **w**, appears in the second term for the **u** retrieval in Equation 3. The second term makes a correction for the effect of the vertical velocity on the radial velocity measured by the oblique beam.
3. A typical value of Θ is 16°, yielding cot(16°) = 3.49 and sec(16°) = 3.63.

Equations for a Turbulent Wind Field

Due to turbulent variations in the winds, $\mathbf{V}_2$ will be affected by the vertical velocity in the b_2-beam, $\mathbf{w}_2$, which may differ from what was observed by the b_1-beam, $\mathbf{w}_1$. Such turbulent variations in the wind will introduce errors in wind speeds retrieved using Equation 3.

Consider the following revised model for the profiler observations:

$$\mathbf{V}_1 = \mathbf{w}_1, \tag{4}$$

$$\mathbf{V}_2 = \mathbf{u}_2 \cdot \sin(\Theta) + \mathbf{w}_2 \cdot \cos(\Theta). \tag{5}$$

The appropriate retrieval equation for the true horizontal wind speed would be

$$\mathbf{u}_2 = \mathbf{V}_2 \cdot \sec(\Theta) - \mathbf{w}_2 \cdot \cot(\Theta). \tag{6}$$

However, in general, $\mathbf{w}_2$ is not observed. It is usually approximated by $\mathbf{w}_1$, as in the following equation for estimating wind speed:

$$\mathbf{u}_{ret} = \mathbf{V}_2 \cdot \sec(\Theta) - \mathbf{w}_1 \cdot \cot(\Theta) \tag{7}$$

The retrieved wind speed can be expressed as the true wind plus an error term, by combining Equations 6 and 7.

$$\mathbf{u}_{ret} = \mathbf{u}_2 + (\mathbf{w}_2 - \mathbf{w}_1) \cdot \cot(\Theta) \tag{8}$$

The error term in Equation 8 is composed of the difference between the vertical velocities over the two beams, amplified by the cotangent(Θ) term. It is useful to note that an error term would also exist in Equation 8 for a retrieval algorithm that did not correct for vertical velocity in Equation 7. Instantaneous retrieved wind speeds will be affected by the error term because turbulent eddies cause the vertical velocity to vary rapidly in time and space. As a result, the retrieved wind speed will be more variable than the true wind speed. However, the long term average of the retrieved wind speed will be unbiased with respect to the true wind speed if the average value of the error term is zero. Also the retrieved average wind speed will be close to the true average wind speed when the averaging interval is long, compared to the space/time-scale of variability in the vertical wind.

On the other hand, retrievals of the peak wind speed during an interval may be systematically biased if positive peaks in the error term occur at the same time, or nearly the same time, as true wind speed peaks. The probability of such coincidence would increase under three conditions: 1) As the averaging interval becomes long, 2) As the time-scale of vertical wind variability becomes short compared to the time-interval between observations, or 3) As the distance between the beams becomes large compared to the spatial scale of the turbulent eddies. Some quantitative insights into these potential errors of retrieved peak wind speeds can be obtained by use of a statistical model, as described in Section 4.2, to simulate Doppler profiler observations and the resulting retrieved wind speeds.

4.2. A Statistical Model for Simulating Profiler Observations

Profiler observations can be simulated by modeling the horizontal and vertical wind speeds with first-order auto-regressive (AR1) process models. For simulating time series of the horizontal wind velocity consider the following (Wilks 1995):

$$U(t) = \alpha \cdot U(t-1) + \beta \cdot Z_U(t) + \gamma \tag{9}$$

where time is denoted by **t**, and **U(t)** is the horizontal wind speed over the b_2-beam, α, β, and γ are the model parameters, and α is less than or equal to 1. The random variable $\mathbf{Z_U}$ has a normal distribution with a mean of zero and a standard deviation of one. The autocorrelation function (ACF) of the process is exponential in form, characterized by α:

$$\mathbf{ACF(U(t))= \exp(-t/\tau_0),} \tag{10}$$

where $\tau_0 = -1/\ln(\alpha)$ resulting in

$$\mathbf{ACF(U(t))= \alpha^{|t|}.} \tag{11}$$

The expected value of the process is determined by α and γ by

$$\mathbf{E[U] = \gamma \cdot [1+\alpha/(1-\alpha)],} \tag{12}$$

and the variance of the process is determined by α and β:

$$\mathbf{Var[U] = \beta^2 \cdot [1/(1-\alpha^2)].} \tag{13}$$

Table 2 gives realistic parameter values for simulating 1-second horizontal wind speed data with five-minute averaging (Merceret 1995). Set 1 applies to an average wind speed of 10 kts with an average peak speed of 14.1 kts, while the average and peak wind speeds from set 2 are 20 and 28.2 respectively. The 5th parameter gives the standard deviation of the wind speed or the square root of the variance.

Table 2. Parameter values for realistic wind speed distributions.

Parameter	*Set 1*	*Set 2*
α	0.9	0.9
β	0.7	1.4
γ	1.0	2.0
E[U]	10	20
$(Var\ [U])^{1/2}$	1.606	3.212
Average Peak Speed	~14.1	~28.2

Note that the average peak wind speed in Table 2 is a factor of 1.41 times the average wind speed (E[U]). This "gust" factor is consistent with previous empirical studies of peak winds (Lambert 2002). The average peak wind speed was determined empirically from a Monte Carlo simulation of 1000 five-minute intervals of 300 1-second observations in each interval. The simulation was done using the statistical package S-PLUS® (Insightful Corporation 2000). The Appendix at the end of this report outlines an analytical approach to determining statistics of the average peak wind speed.

An AR1 model in the form of Equation 9 was assumed for the vertical velocity over the b_1-beam:

$$W(t) = A \cdot W(t\text{-}1) + B \cdot Z_W(t) + C \qquad (14)$$

First-guess parameters for the AR1 model in Equation 14 were derived from an analysis of DmSS vertical velocity statistics from 9 January 2003. High temporal resolution vertical velocity data were obtained for several hours after sunrise from Mr. Scott Barney of Boeing. The time interval between the vertical velocity observations was 2.58 seconds. At this time lag the correlation of the vertical velocity was 0.48 and its overall standard deviation at altitudes above 200 ft was ~0.60 kts. The following parameters are applicable for the AR1 model described by Equation 14: $\mathbf{A} = 0.75$, $\mathbf{B} = 0.40$, $\mathbf{C} = 0.0$. Using **W** from Equation 14 in Equations 12 and 13, the resultant mean and variance are $\mathbf{E[W]} = 0.0$, and $\mathbf{Var[W]} = 0.36\ (\text{kts})^2$.

A simple method for determining the magnitude of the error term in Equation 8 is to use the AR1 models in Equations 9 and 14 to simulate $\mathbf{V_1(t)}$ and $\mathbf{V_2(t)}$. Vertical velocities $\mathbf{W_1}$ and $\mathbf{W_2}$ are obtained from **W(t)** and **W(t+1)**, respectively. This is equivalent to assuming that **W** is uniform in space but varying in time, and that the profiler samples the beams alternately at a time interval of 1 second. As a result there is a 1-second difference between the time of the **W**-value used in the wind speed retrieval, $\mathbf{W_1}$, and the **W**-value used in the profiler simulation of $\mathbf{V_2(t)}$ over the b_2-beam, $\mathbf{W_2}$.

Figure 16 shows a scatter diagram of true wind speeds versus retrieved wind speeds from a Monte Carlo simulation using Equations 9 and 14, along with Equations 4, 5, 6 and 7. For each second of the 170-minute simulation true horizontal and vertical wind speeds were generated from equations 9 and 14, respectively. Simulated profiler observations V_1 and V_2 were then generated from Equations 4 and 5. The true wind speed was derived from Equation 6 and a retrieved wind speed was derived from Equation 7. For every 5-minute interval average and peak wind speed were derived from the 1-second resolution true and retrieved wind speeds.

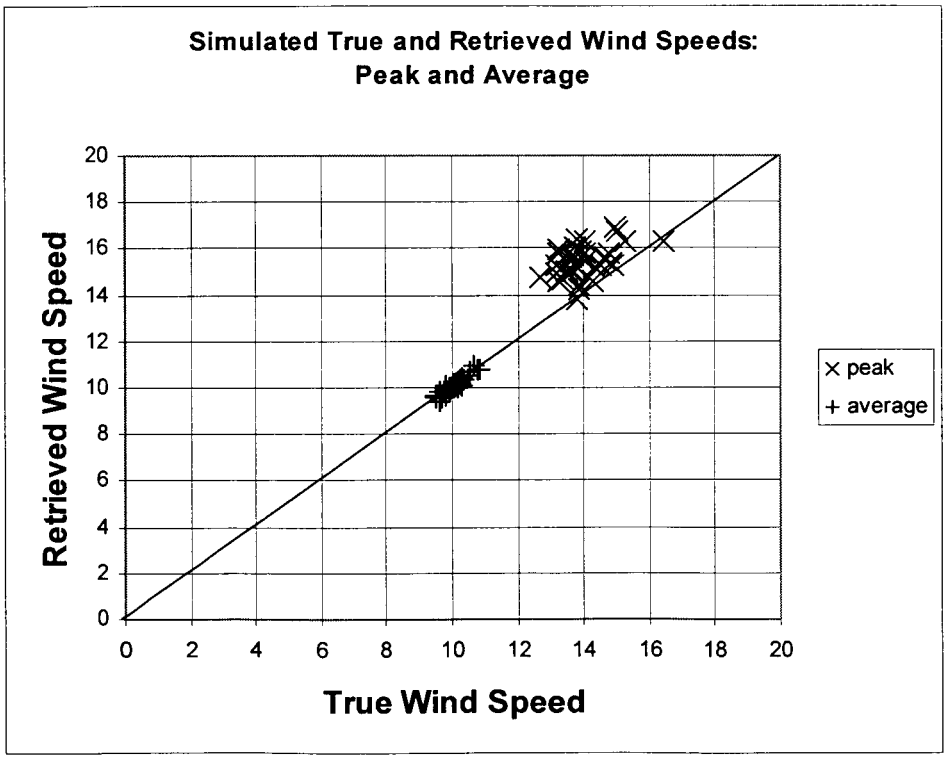

Figure 16. True versus retrieved wind speeds from a 170-minute simulation of 10 200 1-second values, with a sample-size of 300, representing 5-minute averages There are 34 pairs of true and retrieved wind speeds for the average wind speed and peak wind speed. A 1:1 ratio line shows the average retrieved wind speed to be unbiased while the peak retrieved wind speeds are biased high on average, usually being above the line.

The Monte Carlo simulation shown in Figure 16 resulted in an unbiased average retrieved wind speed of 10, but a clear bias in the average retrieved peak wind speed of 16.1 as compared to the average true peak wind speed of 14.1, an increase of ~14%. The appendix contains a detailed description of an analytical approach to solving for errors in retrieving peak wind speeds from an idealized Doppler wind profiler.

5. Summary

The goal of this task was to evaluate the performance of an acoustic, phased-array DmSS installed near SLC-37 to be used as a substitute for a tall wind tower. Wind data from the DmSS will be used by the 45 WS LWO to evaluate LCC and to make critical GO/NO GO decisions for the Evolved Expendable Launch Vehicles. Peak wind observations exceeding approximately 15 to 20 kts are critical with regard to ground operations and LCC.

The evaluation was conducted by comparing DmSS wind speed and direction data with similar observations from the nearest tall wind tower, a distance of 0.95 n mi to the SSE and the nearest short wind tower, a distance of 0.6 n mi to the northwest. DmSS data reports were archived every minute, whereas the archive of tower data contained 5-minute averages. Direct comparisons of DmSS and wind tower data were made using 5-minute data from both sources. Because of the turbulent, incoherent nature of wind variations and the distance between the DmSS and tower wind sensors, differences in wind speed and direction were expected and were observed in the high resolution 5-minute data. However, the comparisons of data availability, average wind conditions and peak wind conditions made in this study reveal important aspects of DmSS functionality with respect to wind towers.

5.1. Data Availability

Data availability from the wind towers exceeded 99.7%. DmSS data availability was assessed from the 1-minute DmSS observations, and missing data codes were interpreted as unavailable data. Performance of the SLC-37 DmSS with respect to data availability was found to be consistent with previous studies of acoustic Doppler wind profiling systems and the commercial-off-the-shelf DmSS in particular. The conclusions from this analysis are:

- Overall DmSS data availability at 98 ft, the level to be monitored by the LWO during operations, averaged 90% or better with a marked decrease above that level likely due to atmospheric attenuation of the acoustic signal.
- There was a distinct diurnal cycle in DmSS data availability with a ~15% reduction for several hours around sunrise and sunset. Data drop-outs during these intervals time were sporadic. The diurnal cycle in data availability was caused by weakened atmospheric backscattering of the acoustic signal related to the diurnal cycle in the vertical profile of atmospheric temperature variations near the surface.
- Precipitation also resulted in missing data reports from the DmSS at all levels.

5.2. Average Wind

Performance of the SLC-37 DmSS with respect to 5-minute average wind speeds and directions was found to be consistent with previous studies of acoustic Doppler wind profiling systems and the commercial-off-the-shelf DmSS in particular. Direct comparisons between the DmSS and wind tower data were made from coincident 5-minute averages of each type. The conclusions from this comparison are:

- Wind speed and direction variations associated with coherent meteorological phenomena such as sea breezes were well represented by the DmSS and towers. Direct time-series comparisons of 5-minute wind speeds between the DmSS and wind towers showed some differences, but the differences were not greater than what could be attributed to incoherent, turbulent variations in the wind field.
- The DmSS vertical profile of average wind speed showed good agreement with the wind towers
- The DmSS diurnal cycle of average wind speed showed good agreement with the wind towers.

5.3. Peak Wind

The AMU is not aware of any previous evaluations of peak wind speeds from a DmSS. In the present study systematic differences were found between the DmSS and wind tower 5-minute peak wind speeds. The DmSS peak wind speeds were higher, on average, than the wind tower peak wind speeds by about 25%. The conclusions from this analysis are:

- The vertical profile of DmSS peak wind speeds showed a consistent high bias at all levels.

- The diurnal cycle of DmSS peak wind speeds showed high biases throughout the 24-hour day, with greater over-estimates during the day-time hours.

5.4. Statistical Modeling of the Peak Speed High Bias

A physically-based statistical model of an idealized Doppler wind profiler was developed to aid in the interpretation of DmSS comparisons with wind tower data. The model predicted the following characteristics for wind speed retrievals from a phased-array Doppler profiler:

- Unbiased average wind speeds.
- Positively biased peak wind speeds.
- A positive correlation between the magnitude of the bias in peak wind speeds and the magnitude of variability in the vertical velocity.

The source of the bias in peak wind speeds in the model was in an under-sampling of variations in the vertical velocity field. This under-sampling is consistent with physical characteristics of a phased array system and the real atmosphere: That is, a single beam which is sequentially pointed in vertical and oblique directions to sample vertical and horizontal components of the wind field will miss turbulent variations of the vertical velocity, which are required to accurately retrieve the instantaneous horizontal velocity. As a result the instantaneous retrieved wind speeds can be expressed as the true wind speed plus a random error term. The average retrieved wind speed will be well determined over an interval of time, say 5-minutes, because the random error term averages to near-zero. However, the error term causes the instantaneous retrieved wind speeds to be more variable than the true wind speeds. The increased variability results in a positive bias in the peak retrieved wind speed. The magnitude of the error term increases with an increase in the variability of the vertical velocity, resulting in an increased bias. The model predicted characteristics of an unbiased average speed, a positively biased peak speed and a positive correlation between the bias and the variability of the vertical velocity were observed in the comparison of DmSS and wind tower data.

5.5. Conclusions

This comparative analysis of wind speed and direction data from the DmSS with nearby wind towers confirms the results of previous studies regarding data availability and average wind speed and direction from the phased-array acoustic Doppler wind profiler. The DmSS average wind conditions were consistent with those observed at the towers. DmSS data availability was somewhat less than that from the towers, ~90% versus 99.7%, due to diurnal variations in atmospheric stability and effects of precipitation.

However, peak wind speed observations from the DmSS were biased high with respect to the wind tower observations by about 25%. The source of the high bias appears to be due to an under-sampling of vertical velocity variations by the phased array system, based on idealized mathematical models of the profiler and the wind environment. The models predicted three important characteristics that were also observed in the comparison with wind tower data: 1) An unbiased average wind speed from the profiler, 2) A high bias for peak wind speeds from the profiler. and 3) A positive correlation between the variability of the vertical velocity and the bias.

APPENDIX

Extreme Value Theory and Bias in Peak Wind Speeds

The idealized profiler concept introduced in Section 4 can be used to obtain quantitative insights into the statistics of true peak wind speeds and retrieved peak wind speeds by employing analytical properties of the Gumbel (or Extreme Value Type-I) distribution for maxima.

A Gumbel distribution can be generated by extracting the maximum value from a random sample of normally distributed variables, and repeating the process ad infinitum (Coles 2001). In the present case, variations in "true" wind speed are assumed to be normally distributed. For each random sample of true wind speeds the peak value is selected and used to create a distribution of true peak wind speeds. The distribution of true peak wind speeds will be Gumbel in form. At the same time a sample of retrieved wind speeds is generated consisting of the true wind speed plus an error term as described by Equation 8. A corresponding distribution of retrieved peak wind speeds is also generated by this process. When the error term is also normal and independent of the true wind speed, the resulting distribution of retrieved peak wind speeds will be Gumbel in form with parameters that are different from those of the true peak wind speed distribution. The equations below describe how the resulting Gumbel distribution depends on the parameters of the underlying normal distributions of true wind speed and the error term.

The normal distributions are said to be "in the domain of attraction" of the Gumbel distribution. The distribution of the maxima will converge to the Gumbel probability density function (PDF) as the sample size, n, increases. The Gumbel PDF parameters can be described in terms of n and the parameters of the underlying normal distribution. The solution for the average maximum value can be obtained analytically when the members of the normally distributed sample are independent and un-correlated. The Gumbel PDF is given by

$$G(x) = 1/\lambda \cdot \exp\{-(x-\xi)/\lambda\} \cdot \exp[-\exp\{-(x-\xi)/\lambda\}], \quad \text{(A1)}$$

where λ and ξ are the scale and location parameters, respectively. The expected value and variance of the maxima, **X** in this case, are given by

$$E[X] = \xi + \lambda \cdot 0.5772 \quad \text{and} \quad \text{(A2)}$$

$$\mathbf{Var}\,[X] = \lambda^2 \cdot \pi^2/6, \quad \text{(A3)}$$

respectively. The value 0.5772 is an approximation of Euler's constant (Abramowitz and Stegun 1965), hereafter **Eu**.

When μ and σ are the mean and standard deviation of the normal distribution in the domain of attraction, the parameters of the resulting Gumbel PDF are

$$\xi = \mu + a_n \cdot \sigma \quad \text{and} \quad \text{(A4)}$$

$$\lambda = b_n \cdot \sigma, \quad \text{(A5)}$$

where, a_n and b_n, known as normalization coefficients, are dependent on the sample size and are given by (T. Rolf Turner University of New Brunswick, Canada, personal communication)

$$a_n = \mathrm{sqrt}[2\cdot\ln(n)] - [\ln(4\pi) + \ln(\ln(n))]/[2\cdot\mathrm{sqrt}(2\cdot\ln(n))] \quad \text{and} \quad \text{(A6)}$$

$$b_n = 1/\mathrm{sqrt}[2\cdot\ln(n)]. \quad \text{(A7)}$$

The expected value of the true maxima can then be written in terms of parameters of the underlying normal distribution by

$$E[X_T] = \mu_T + \sigma_T \cdot (a_n + E_u b_n). \quad \text{(A8)}$$

Using the example from (Section 4.2) with $\mu_T = 10$, $\sigma_T = 1.606$, and n=300, we find $\mathbf{a_n} = 2.7541$, $\mathbf{b_n} = 0.2961$, resulting in $\mathbf{E[X_T]} = 14.7$. This expected value of the peak wind from Equation A8 is slightly larger than the Monte Carlo result shown in Figure 16. The average peak wind for the analytically derived solution is weakly dependent on n, the sample size. This suggests that a closer agreement with the Monte Carlo result could be obtained by correcting for the number of independent samples. When the number of independent samples (n) in the analytical solution is decreased from 300 to 100, the average peak wind speed decreases to 14.1. However the standard procedure (Jones 1975) for transforming the number of dependent samples into the number of independent samples by summing over the ACF results in about 16 independent samples (reduced from 300) and an average peak wind speed of about 13.0. Apparently this approach to the problem of independence does not apply here because the correlation tends to produce "clumping" of maxima (Coles 2001). Nevertheless, this comparison between Monte Carlo simulations with correlated variables and the analytical solution for uncorrelated variables indicates that the latter does provide useful, quantitative insights into the distribution of maxima.

Gumbel distribution parameters for the retrieved peak wind speed are made by making use of Equation 8 in Section 4.1, which shows that the average retrieved peak wind speed will be equal to the average true peak wind speed, $\mu_{Ret} = \mu_T$, but that the variability of the retrieved wind speed will be greater than that of the true wind speed because of the error term. It is the increased variability of the retrieved wind speed that contributes to the bias in the average retrieved peak wind speed seen in Figure 16.

From a statistical point-of-view, the additional variability in the retrieved wind speed will be dependent on the variance in the lag-1 difference, **W(t+1) - W(t)**. The residual variance, $\mathbf{Res_{Var}}$, is determined by the lag-1 correlation coefficient, **A** (from Equation 14) and the full variance of **W** as follows:

$$\mathbf{Res_{Var}} = \mathbf{(1-A^2)*Var[W]} \tag{A9}$$

The variance of the retrieved wind is then obtained by summing the variance of the true wind with the product of the residual variance and the square of the amplifying cotangent term:

$$\mathbf{Var_{Ret}} = \mathbf{Var[U]} + \mathbf{Res_{Var}} * \mathbf{Cot^2(\Theta)}. \tag{A10}$$

In this case $\mathbf{Res_{Var}}$ is $(0.3969)^2$ and the variance of the retrieved wind, $\mathbf{Var_{Ret}}$, becomes 4.4980, a 74 % increase over the variance of the true wind.

The expected value for the retrieved peak wind can now be calculated from

$$\mathbf{E[X_{Ret}]} = \mu_T + \sigma_{Ret} * (\mathbf{a_n} + \mathbf{Eu}\ \mathbf{b_n}). \tag{A11}$$

The expected value of the retrieved peak wind from Equation A10 becomes 16.2. The retrieved peak wind speed is ~10% higher than the true peak wind speed, remarkably consistent with the Monte Carlo result shown in Figure 16.

Figure A1 shows modeled probability density functions (pdfs) of wind speeds for the case where the Gaussian, or normal, distribution in the domain of attraction has a mean of 10 and a standard deviation of 1.56. The true distribution of peak winds is shown for a sample size of 100, giving an average peak wind of 14 kt and a gust factor of 1.4. The retrieved peak wind distribution has an average of 16.8 kt and a bias of 20%. The standard deviation of vertical velocity is 0.64 kt, equivalent to a residual variance of 0.41 kt^2.

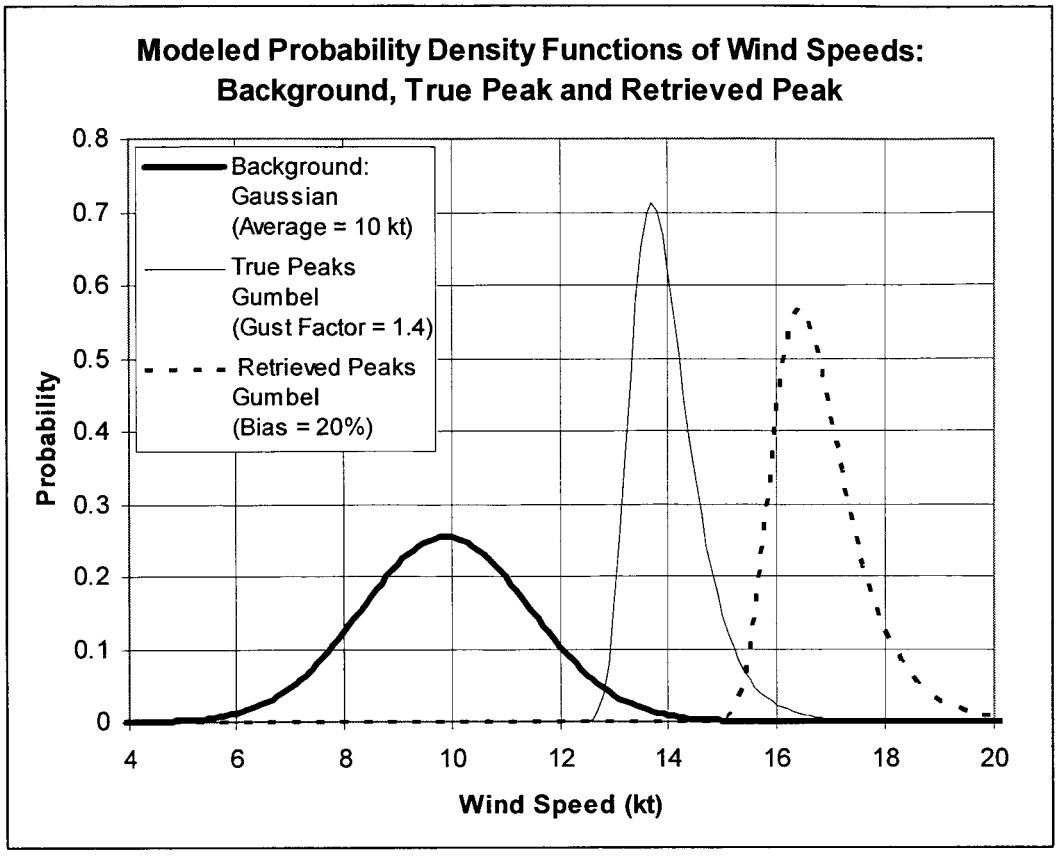

Figure A1. Modeled pdfs of wind speeds illustrating Gumbel distributions of true and retrieved peaks derived from a background distribution that is Gaussian. Distribution parameters have been chosen to give an average background wind of 10 kt, a gust factor of 1.4 for the true peaks and a bias of 20% for the retrieved peaks.

The influence of the residual variance, $\mathbf{Res_{Var}}$, in enhancing the average retrieved peak wind speed above that of the average true peak wind speed can be visualized by graphing the percent bias of $\mathbf{E[X_{Ret}]}$ in a two-dimensional coordinate system of μ_T versus $(\mathbf{Res_{Var}})^{1/2}$. For this example it is assumed that the gust factor is 1.4, independent of μ_T, the true average wind speed. Contours of the percent-bias,

$$\mathbf{\%Bias} = 100*(\mathbf{E[X_{Ret}]} - \mathbf{E[X_T]})/\mathbf{E[X_T]} \qquad \text{(A12)}$$

are straight lines as shown in Figure A2.

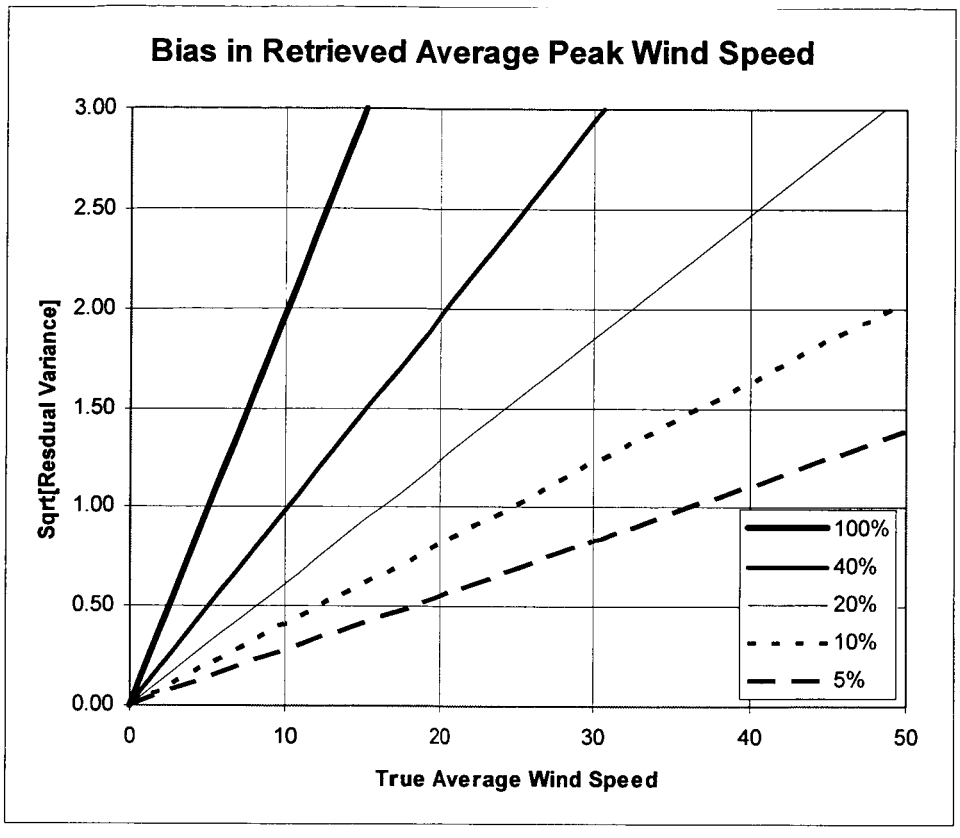

Figure A2. The bias in retrieved average peak wind speed as a function of true average wind speed and the square root of the residual variance in the vertical velocity, based on the analytical models for wind speed and vertical velocity presented above.

References

Abramowitz, M., and I. A. Stegun, 1965: Handbook of Mathematical Functions. Dover Publications, Inc., New York, 1046 pp.

AeroVironment, Inc., 2001: Doppler MiniSODAR™ System, Operation and Maintenance Manual, Version 1.5, 53 pp.

Barthelmie, R. J., L. Folkerts, F. T. Ormel, P. Sanderhoff, P. J. Eecen, O. Stobbe, and N. M. Nielsen, 2003: Offshore wind turbine wakes measured by SODAR. J. Atmos. Oceanic Tech., 20, 466-477.

Coles, S., 2001: An Introduction to Statistical Modeling of Extreme Values, Springer Series in Statistics, 208 pp.

Crescenti, G. H., 1999: A Study to Characterize Performance Statistics of Various Ground –Based Remote Sensors. NOAA Tech. Mem. ERL ARL-229, 286 pp.

Crescenti, G. H., 1998: The degradation of Doppler SODAR performance due to noise: A review. *Atmos. Env.*, **32**, 1499-1509.

Crescenti, G. H., 1997: A look back at two decades of Doppler SODAR comparison studies. Bull. Amer. Meteor. Soc., 78, 651-673.

Hall, F. F., Jr., J. G. Edinger, W. D. Neff, 1975: Convective plumes in the planetary boundary layer, investigated with an acoustic sounder. *J. Appl. Meteorology*, **14**, 513-523.

Insightful Corporation, 2000: S-PLUS® 6 User's Guide, Insightful Corp., Seattle, WA, 470 pp.

Jones, R. H., 1975: Estimating the variance of time averages. J. Appl. Meteor., 14, 159-163.

Lambert, W. C., 2002: Statistical short-range guidance for peak wind speed forecasts on Kennedy Space Center/Cape Canaveral Air Force Station: Phase I Results. NASA Contractor Report CR-2002-211180, Kennedy Space Center, FL, 39 pp. [Available from ENSCO, Inc., 1980 N. Atlantic Ave., Suite 230, Cocoa Beach, FL, 32931.]

Merceret, F. J., 1995: The effect of sensor sheltering and averaging techniques on wind measurements at the Shuttle Landing Facility. NASA TM-111262, 42 pp. [Available from the NASA Center for Aerospace Information, 7121 Standard Drive, Hanover, MD 21076-1320]

Peterson, V. L., 1988: Wind Profiling: The History, Principles, and Applications of Clear-Air Doppler Radar. Tycho Technology, Inc., Boulder, CO, 66 pp.

Wilks, D. S., 1995: Statistical Methods in the Atmospheric Sciences. Academic Press, Inc., San Diego, CA, 467 pp.

WMO, 1983: Guide to Meteorological Instruments and Methods of Observation. World Meteorological Organization No. 8, 5th edition, Geneva, Switzerland.

Wyngaard, J. C., 1973: On surface-layer turbulence. *Workshop on Micrometeorology*, D. A. Haugen, Ed., Amer. Meteor., Soc., 101-149.

List of Acronyms

45 WS	45th Weather Squadron
ACF	Autocorrelation Function
AMU	Applied Meteorology Unit
AR1	Autoregressive model of the first order
BOA	Boulder Atmospheric Observatory
CCAFS	Cape Canaveral Air Force Station
CSR	Computer Sciences Raytheon
DmSS	Doppler MiniSODAR™ System
KSC	Kennedy Space Center
LCC	Launch Commit Criteria
LWO	Launch Weather Officer
NOAA	National and Oceanic Atmospheric Administration
PC	Personal Computer
PDF	Probability Density Function
RWO	Range Weather Operations
SLC	Space Launch Complex
SNR	Signal-to-Noise Ratio
UTC	Universal Coordinated Time
WMO	World Meteorological Organization

NOTICE

Mention of a copyrighted, trademarked or proprietary product, service, or document does not constitute endorsement thereof by the author, ENSCO, Inc., the AMU, the National Aeronautics and Space Administration, or the United States Government. Any such mention is solely to inform the reader of the resources used to conduct the work reported herein.

REPORT DOCUMENTATION PAGE

Form Approved
OMB No. 0704-0188

1. AGENCY USE ONLY (Leave blank)	2. REPORT DATE	3. REPORT TYPE AND DATES COVERED
	October 2003	Contractor Report

4. TITLE AND SUBTITLE
MiniSODAR™ Evaluation

5. FUNDING NUMBERS
C-NAS10-01052

6. AUTHOR(S)
David A. Short, Mark M. Wheeler

7. PERFORMING ORGANIZATION NAME(S) AND ADDRESS(ES)
ENSCO, Inc., 1980 North Atlantic Avenue, Suite 230, Cocoa Beach, FL 32931

8. PERFORMING ORGANIZATION REPORT NUMBER
03-003

9. SPONSORING/MONITORING AGENCY NAME(S) AND ADDRESS(ES)
NASA, John F. Kennedy Space Center, Code YA-D, Kennedy Space Center, FL 32899

10. SPONSORING/MONITORING AGENCY REPORT NUMBER
NASA/CR-2003-211192

11. SUPPLEMENTARY NOTES
Subject Cat.: #47 (Meteorology and Climatology)

12A. DISTRIBUTION/AVAILABILITY STATEMENT
Unclassified - Unlimited

12B. DISTRIBUTION CODE

13. ABSTRACT (Maximum 200 Words)

This report describes results of the AMU's Instrumentation and Measurement task for evaluation of the Doppler miniSODAR™ System (DmSS). The DmSS is an acoustic wind profiler providing high resolution data to a height of ~ 410 ft. The Boeing Company installed a DmSS near Space Launch Complex 37 in mid-2002 as a substitute for a tall wind tower and plans to use DmSS data for the analysis and forecasting of winds during ground and launch operations. Peak wind speed data are of particular importance to Launch Weather Officers of the 45th Weather Squadron for evaluating user Launch Commit Criteria.

The AMU performed a comparative analysis of wind data between the DmSS and nearby wind towers from August 2002 to July 2003. The DmSS vertical profile of average wind speed showed good agreement with the wind towers. However, the DMSS peak wind speeds were higher, on average, than the wind tower peak wind speeds by about 25%. A statistical model of an idealized Doppler profiler was developed and it predicted that average wind speeds would be well determined but peak wind speeds would be over-estimated due to an under-specification of vertical velocity variations in the atmosphere over the profiler.

14. SUBJECT TERMS
Wind Profiler, Instrument Evaluation, Peak Winds, Launch Commit Criteria

15. NUMBER OF PAGES 34

16. PRICE CODE

17. SECURITY CLASSIFICATION OF REPORT	18. SECURITY CLASSIFICATION OF THIS PAGE	19. SECURITY CLASSIFICATION OF ABSTRACT	20. LIMITATION OF ABSTRACT
UNCLASSIFIED	UNCLASSIFIED	UNCLASSIFIED	NONE